

Microstrip Dyadic 표면 Green 함수의 근사표현식

正會員 崔 翼 權*

An Approximate Closed Form Representation
of the Microstrip Dyadic Surface Green's FunctionIkguen Choi* *Regular Member*

要 約

접지면이 있는 무한 평판의 유전체상에 놓인 점 전기전류원 문제에서 야기되는 마이크로스트립 표면 dyadic Green 함수에 대한 간단하면서도 정확한 근사표현식이 본 논문에서 개발된다. 이 근사표현식은 본 논문에서 소개하는 새로운 방법에 의해서 유도된 공간파와 표면파 그리고 전이지역에서 이들간의 결합을 나타내는 전이함수를 모두 포함하고 있으며, 유전체 두께가 0.04λ (λ 는 자유공간파장)나 되는 두꺼운 경우에도 점원에서 0.1λ 떨어진 가까운 위치에서까지 유용하므로 실제 마이크로스트립 안테나 어레이 설계시 안테나 소자간 전자기적 결합에 의한 어레이 안테나의 특성저하나 마이크로웨이브회로 또는 초고속의 디지털프린트 회로기판 설계시 연결선 특성임피던스와 연결선간의 crosstalk에 의한 회로성능 저하 문제를 해석하는데 아주 유효하다. 이 근사식에 의한 상호임피던스 수치해석 결과와 함께 계산에 소요되는 CPU 시간을 예시함으로써 본 근사식의 정확성 및 효율성을 입증하여 보았다.

ABSTRACT

A simple closed form approximation is developed by a new approach presented in this paper for the microstrip surface dyadic Green's function which arises in the problem of an electric current point source on an infinite planar grounded dielectric substrate. This closed form approximation includes the effects of the space wave, the surface wave and their coupling within the transition region near the source, and remains accurate as near as $0.1 \lambda_1$ from the source point for a substrate thickness as large as $0.04 \lambda_1$, where, λ_1 is the free space wavelength. This result can significantly facilitate the rigorous moment method analysis of microstrip antenna arrays on relatively thin substrates of practical interest. Numerical results illustrating the accuracy of the closed form approximation are presented and CPU times associated with some mutual impedance calculations are also included.

*韓國電子通信研究所
ETRI
論文番號 : 93-56

I. Introduction

A rigorous moment method analysis of microstrip antenna arrays generally employs a microstrip dyadic surface Green's function in the formulation of the integral equation for the currents induced on the microstrip array elements by an appropriate feed^(1,2). That integral equation can be solved numerically via the moment (MM) to yield useful design data such as the input impedance, reflection coefficient, active-element pattern, efficiency and mutual coupling between microstrip antenna element^(3,4). However, if the conventional Sommerfeld type integral representation of the microstrip surface Green's function is employed, then due to the slow convergence of that integral representation for laterally separated source and field points, the rigorous MM solution becomes rather inefficient. Thus, in this paper, simple but accurate closed form approximations for these integrals representing the microstrip surface Green's functions are derived. The closed form approximations include the effects of the space wave, the surface wave and their coupling within the transition region near the source. The space wave is derived by a new approach developed in this paper. This approach uses the Hankel transform representations and is largely based on the physical consideration of the outgoing wave radiation condition.

In Section II, the microstrip surface Green's function is presented in terms of the pertinent Sommerfeld type integrals. In Section III, an approximate closed form representation of the microstrip surface Green's function is derived via a new approach introduced in this paper, and in Section IV, their excellent accuracy is illustrated by comparison with the exact numerical integration results.

In the following, the time convention $\exp(j\omega t)$ is assumed and suppressed.

II. Microstrip Dyadic Surface Green's Function

The term "microstrip dyadic surface Green's function" is used in this paper to name a dyadic quantity $\bar{\bar{G}}$ in terms of which the vector electric field \bar{E} on the air-dielectric interface is evaluated by

$$\bar{E}(\bar{r}) = -j\omega\mu_1 \int_s \bar{\bar{G}}(\bar{r}, \bar{r}') \cdot \bar{J}(\bar{r}') ds \quad (1)$$

In the above, \bar{J} means an electric current density source of \bar{E} . \bar{r} and \bar{r}' denote the position vectors from the origin of the coordinate system to the observation points and source points, respectively. ω denotes the angular frequency and μ_1 denotes the permeability of the air. The source and observation points in(1) are limited on the air-dielectric interface where $z=0$ as is the case of special interest in the MM analysis of microstrip antenna arrays. Therefore, we need to consider only the 4-components G_{xx} , G_{xy} , G_{yx} and G_{yy} of $\bar{\bar{G}}$ which are associated with the tangential electric field at $z=0$ due to a tangential current.

The above 4-components can be obtained from the knowledge of the electric field at $z=0$ due to a point electric current source of strength $\bar{P}_e(\bar{P}_e = \hat{x}P_{ex} + \hat{y}P_{ey})$, which is located on the dielectric surface as shown in Figure 1.

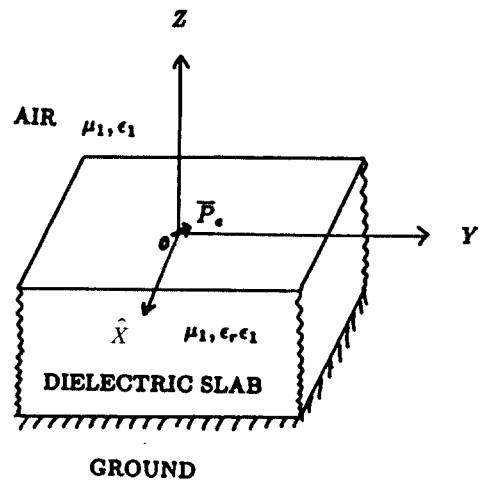


Figure 1. Point electric current source of strength $\bar{P}_e = x\hat{P}_{ex} + y\hat{P}_{ey}$ on an infinite grounded dielectric slab.

The field due to $\bar{P}_e \delta(r')$, where δ is the dirac delta function, can be obtained via the conventional magnetic vector potential method⁽⁵⁾ and the resulting representations of the microstrip dyadic surface Green's function is

$$G_{xx} = \frac{1}{\mu_1 k_1^2} (k_1^2 A_x + \frac{\partial^2}{\partial x^2} A_x + \frac{\partial^2}{\partial x^2} A_z) \quad (2)$$

$$G_{xy} = \frac{1}{\mu_1 k_1^2} (\frac{\partial^2}{\partial x \partial y} A_x + \frac{\partial^2}{\partial x \partial y} A_z) \quad (3)$$

$$G_{yx} = G_{xy} \quad (4)$$

$$G_{yy} = \frac{1}{\mu_1 k_1^2} (k_1^2 A_x + \frac{\partial^2}{\partial y^2} A_x + \frac{\partial^2}{\partial y^2} A_z) \quad (5)$$

where

$$A_x(\rho) = \frac{\mu_1}{2\pi} \int_0^\infty \frac{k_\rho J_0(k_\rho \rho)}{D_{TE}} dk_\rho \quad (6)$$

$$A_z(\rho) = \frac{\mu_1}{2\pi} (\epsilon_r - 1) \int_0^\infty \frac{k_{z1} k_\rho J_0(k_\rho \rho)}{D_{TE} D_{TM}} dk_\rho \quad (7)$$

or

$$A_x(\rho) = \frac{\pi_1}{4\pi} \int_\infty^\infty \frac{k_\rho H_0^{(2)}(k_\rho \rho)}{D_{TE}} dk_\rho \quad (8)$$

$$A_z(\rho) = -\frac{\pi_1}{4\pi} (\epsilon_r - 1) \int_\infty^\infty \frac{k_{z1} k_\rho H_0^{(2)}(k_\rho \rho)}{D_{TE} D_{TM}} dk_\rho \quad (9)$$

and

$$\rho = |\bar{r} - \bar{r}'| = \sqrt{(x-x')^2 + (y-y')^2} \quad (10)$$

$$D_{TE} = jk_{z1} + k_{z2} \cot(k_{z2}d) \quad (11)$$

$$D_{TM} = \epsilon_r k_{z1} + jk_{z2} \tan(k_{z2}d) \quad (12)$$

$$k_{z1} = \sqrt{k_1^2 - k_\rho^2}; \text{Re}(k_{z1}) > 0, \text{Im}(k_{z1}) < 0 \quad (13)$$

$$k_{z2} = \sqrt{\epsilon_r k_1^2 - k_\rho^2}; \text{Re}(k_{z2}) > 0, \text{Im}(k_{z2}) < 0 \quad (14)$$

In the above, $k_1^2 = \omega^2 \mu_1 \epsilon_1$ and ϵ_1 denotes the permittivity of the air.

In practical microstrip antenna structure, the dielectric substrate is electrically thin⁽⁶⁾. Thus, only the TM surface mode wave is assumed to exist for convenience throughout this paper.

III. An Approximate Closed Form Representation for the Microstrip surface Green's Function

For relatively large values of $k_1 \rho$, the integral field representations, A_x and A_z may be approxi-

ated asymptotically by the saddle-point integration method after the Hankel functions in the integrands of (8-9) are replaced by the first-order large-argument approximation. However, the asymptotic approximation is found by the author not to be accurate enough to be applied for rigorous MM analysis of microstrip antenna arrays.

In the following subsections, the pertinent integrals A_x and A_z are approximated in closed forms by a new approach developed in this paper. This approach is largely based on the physical consideration of the outgoing wave radiation condition for $k_1 \rho \rightarrow \infty$ and utilizes the electrically thin dielectric condition to obtain as accurate a closed form approximation as possible, even for the very close vicinity of the source. First A_x will be approximated in Part 1 of this section and then A_z will be approximated in Part 2.

1. A Closed Form Approximation of the Integral for A_x

The intergral field representation for A_x in (6) consists of only the continuous spectrum, i.e., the radiation field. Thus, the asymptotic approximation for the integral in (6) is expected to represent the radiation field but not the bound surface wave field which is also present on this structure; the latter is included in A_z through the presence of a surface wave pole in its integrand. When we separate the integral into three sub-integration intervals, i. e.,

$$0 < k_\rho < k_1 \quad (15)$$

$$k_1 < k_\rho < k_2 \quad (16)$$

$$k_2 < k_\rho, \quad (17)$$

it is easily seen that the imaginary part of this radiation field $\text{Im}(A_x)$ comes mathematically from the integration interval $0 < k_\rho < k_1$ and is given by

$$\text{Im}(A_x) = \frac{\mu_1}{2\pi} \int_0^{k_1} \text{Im}\left(\frac{1}{D_{TE}}\right) k_\rho J_0(k_\rho \rho) dk_\rho \quad (18)$$

It is assumed that the dielectric constant ϵ_r is real. After employing the transformation

$$k_\rho = k_1 t \tag{19}$$

$I_m(A_x)$ is rewritten by

$$I_m(A_x) = \frac{\mu_1 k_1}{2\pi} \int_0^1 F_A(t) t \sqrt{1-t^2} J_0(k_1 \rho t) dt \tag{20}$$

where

$$F_A(t) = \left[I_m \left(\frac{1}{D_{TE}} \right) \right]_{k_\rho = k_1 t} \\ = - \frac{\sin^2 k_1 \sqrt{\epsilon_r - t^2} d}{(\epsilon_r - t^2) \cos^2 k_1 \sqrt{\epsilon_r - t^2} d + (1-t^2) \sin^2 k_1 \sqrt{\epsilon_r - t^2} d} \tag{21}$$

Since, in microstrip antenna application, we may assume that $k_1 d \sqrt{\epsilon_r - t^2} \ll 1$ in the integration interval $0 < t < 1$, F_A in (21) can be approximated as follows :

$$F_A(t) \approx C_0 \sum_{n=0}^{\infty} A_n (1-t^2)^n \tag{22}$$

with

$$C_0 = \frac{(k_1 d)^2}{1 - (\epsilon_r - 1) (k_1 d)^2} \tag{23}$$

$$A_0 = 1 - \frac{1}{3} (k_1 d)^2 (\epsilon_r - 1) + \frac{1}{36} (k_1 d)^4 (\epsilon_r - 1)^2 \tag{24}$$

$$A_1 = -\frac{1}{3} (k_1 d)^2 + \frac{1}{18} (k_1 d)^4 (\epsilon_r - 1) \tag{25}$$

$$A_2 = \frac{1}{36} (k_1 d)^4 \tag{26}$$

In obtaining the above approximation in (22) together with (23) through (26), the following simplifications were introduced :

$$\cos^2 k_1 \sqrt{\epsilon_r - t^2} d \approx 1 \tag{27}$$

$$\sin^2 k_1 \sqrt{\epsilon_r - t^2} d \approx (k_1 d)^2 (\epsilon_r - t^2) \cdot \left\{ 1 - \frac{1}{6} (k_1 d)^2 (\epsilon_r - t^2) \right\}^2 \tag{28}$$

Now substituting (22) into (20) and using the integration formula

$$\int_0^1 x^{\nu+1} (1-x^2)^\mu J_\nu(bx) dx = 2^\mu \Gamma(\mu+1) b^{-(\mu+1)} J_{\nu+\mu+1}(b) \\ (b > 0, \operatorname{Re} \nu > -1, \operatorname{Re} \mu > -1) \tag{29}$$

yields

$$I_m(A_x) = -\frac{\pi_1 k_1}{2\pi} C_0 \sum_{n=0}^{\infty} A_n (2)^{n+1/2} \Gamma(n + \frac{1}{2} + 1) \\ (k_1 \rho)^{-(n+1/2+1)} J_{(n+1/2+1)}(k_1 \rho) \tag{30}$$

In the above, Γ denotes the Gamma function ; also note that the Bessel function in (29) is of fractional order. With the help of the following identity

$$j_n(z) = \sqrt{\frac{\pi}{2z}} J_{n+1/2}(z), \tag{31}$$

where $j_n(z)$ represents the spherical Bessel function of the first kind, and the relations

$$j_n(z) = f_n(z) \sin z + (-1)^{n+1} f_{-n-1}(z) \cos z \\ f_0(z) = z^{-1}, f_2(z) = z^{-2} \\ f_{-n-1}(z) + f_{n+1}(z) = (2n+1)z^{-1} f_n(z) \\ (n=0, \pm 1, \pm 2, \dots) \tag{32}$$

we find following expression for $I_m(A_x)$

$$I_m(A_x) = \frac{\mu_1 k_1}{2\pi} C_0 \left[-\sin k_1 \rho \left\{ \frac{C_3}{(k_1 \rho)^3} + \frac{C_5}{(k_1 \rho)^5} + \frac{C_7}{(k_1 \rho)^7} \right\} \right. \\ \left. + \cos k_1 \rho \left\{ \frac{C_2}{(k_1 \rho)^2} + \frac{C_4}{(k_1 \rho)^4} + \frac{C_6}{(k_1 \rho)^6} \right\} \right] \tag{33}$$

where

$$C_2 = A_0 \qquad C_3 = A_0 - 3A_1 \\ C_4 = 9A_1 - 15A_2 \qquad C_5 = 9A_1 - 90A_2 \\ C_6 = 225A_2 \qquad C_7 = 225A_2 \tag{34}$$

It is noted that $C_0, C_2, C_3, C_4, \dots, C_7$ are all real if the dielectric is lossless. For the present, let it be assumed that the dielectric is lossless ; this condition will be relaxed shortly ; consequently, since (33) furnishes the imaginary part of A_x and it is known from physical considerations that A_x must satisfy the outgoing wave radiation condition for $k_1 \rho \rightarrow \infty$, it is therefore possible to deduce A_x heuristically from $I_m(A_x)$ by simply replacing

$$-\sin k_1 \rho \text{ with } e^{-jk_1 \rho} \tag{35}$$

and likewise by replacing

$$\cos k_1 \rho \text{ with } e^{-jk_1 \rho} \quad (36)$$

Thus, the result for A_x is given by :

$$A_x \approx \frac{\mu_1 k_1}{2\pi} C_0 e^{-jk_1 \rho} \sum_{n=2}^7 \frac{D_n}{(k_1 \rho)^n} \quad (37)$$

where

$$\begin{aligned} D_2 &= jC_2 = jA_0 & D_3 &= C_3 = A_0 - 3A_1 \\ D_4 &= jC_4 = j(9A_1 - 15A_2) & D_5 &= C_5 = 9A_1 - 90A_2 \\ D_6 &= jC_6 = j225A_2 & D_7 &= C_7 = 225A_2 \\ D_8 &= jC_8 = j225A_2 & D_7 &= C_7 = 225A_2 \end{aligned} \quad (38)$$

The corresponding results for the lossy dielectric case can now be obtained directly from(37) via analytic continuation by making ϵ_r in that expression complex to account for loss. It is seen in the next section, that numerical results based on (37) are indeed very accurate even for ρ as small as $0.1 \lambda_1$ (λ_1 = free space wavelength) and it is also seen that (37) gives good results if the dielectric is lossy thereby lending confidence to the present approach.

2. A Closed Form Approximation of the Integral for A_z

Unlike A_x , the Sommerfeld type integral of A_z in (7) yields both a surface (or pole) wave and a continuous (or radiation field) spectrum contribution to the field. However, as is well Known, the solution for surface wave is easily obtained by calculating the residue of the integrand at the pole. The continuous(or radiation) spectral contribution may be approximated in a manner similar to that employed previously for A_x after D_{TM} in the integrand of (7) is approximated as follows using the small argument approximation for sinusoidal functions :

$$\begin{aligned} D_{TM} &= \frac{\cos k_1 \sqrt{\epsilon_r - t^2} d}{(\epsilon_r \sqrt{1-t^2} \cos k_r \sqrt{\epsilon_r - t^2} d + j \sqrt{\epsilon_r - t^2} \sin k_1 \sqrt{\epsilon_r - t^2} d)} \\ &\approx \frac{1}{\epsilon_r^2} \left(-jk_1 d + \frac{\epsilon_r}{\sqrt{1-t^2}} \right) \end{aligned} \quad (39)$$

The pole and continuous spectral wave contribution can be treated distinctly only outside the so-called surface (pole) wave transition region⁽⁷⁾ ; however, within this transition region which exists in the near field of the microstrip patch it is necessary to include the interaction between these two different waves because the pole and continuous spectral waves exhibit a coupling effect⁽⁷⁾ within the transition region where the effects no longer distinct. Mathematics related to the field description within the transition region is available in.⁽⁸⁾ Carrying out the necessary calculations yields the following closed form approximation for the integral

$$\begin{aligned} A_z &= -2\pi jR \\ &+ \frac{\mu_2 k_1}{2\pi} \frac{C_0}{\epsilon_r^2} (\epsilon_r - 1) e^{-jk_1 \rho} \sum_{n=2}^7 \frac{e_n}{(k_1 \rho)^n} \\ &+ \left[-j \pi H_0^{(2)}(k_1 \rho) R \cdot w(b \sqrt{k_1 \rho}) + \frac{e^{-jk_1 \rho}}{k_1 \rho} \cdot \sqrt{2j} \frac{R}{b} \right] \end{aligned} \quad (40)$$

where R is the residue of the integrand of (9) at the pole $k_p = \lambda_p$ and

$$\begin{aligned} e_2 &= j d_0 & e_3 &= d_0 - 3d_1 \\ e_4 &= j(9d_1 - 15d_2) & e_5 &= 9d_1 - 90d_2 \\ e_6 &= j 225d_2 & e_7 &= 225d_2 \\ d_n &= \epsilon_r A_n + b_n ; & n &= 0, 1, 2 \\ b_0 &= 1 - 2/3(k_1 d)^2 (\epsilon_r - 1) + 2/15(k_1 d)^4 (\epsilon_r - 1)^2 \\ b_1 &= 2/3(k_1 d)^2 + 4/15(k_1 d)^4 (\epsilon_r - 1)^2 \\ b_2 &= 2/15(k_1 d)^4 \\ b &= \sqrt{-j + j \frac{\lambda_p}{k_1}} \\ w(z) &= e^{-z^2} \operatorname{erfc}(z) \end{aligned} \quad (41)$$

In the above, the first term represents the non-radiation or bound surface wave, the second sum represents the radiation field contribution, and the third one represents the transition function describing the interaction between the radiation field and the surface wave field. As briefly mentioned before, the term was obtained partly heuristically by applying the uniform saddle point integration method to the integral representation for A_z of (9) as discussed in Felsen and Marcuvitz⁽⁸⁾.

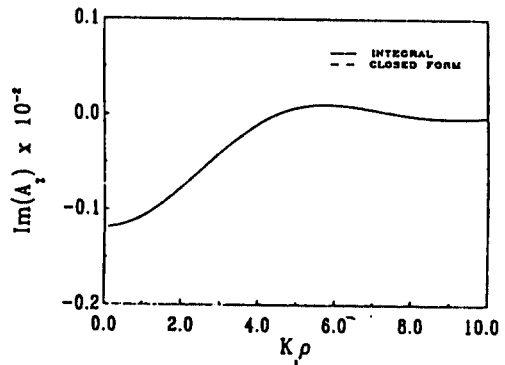
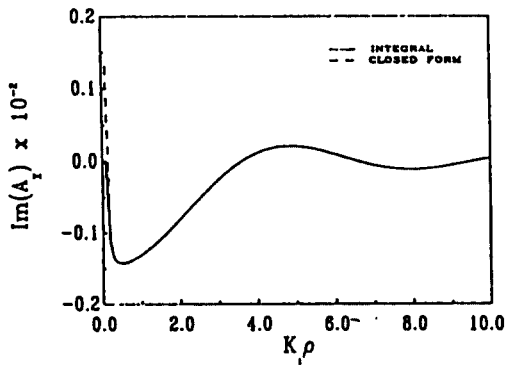
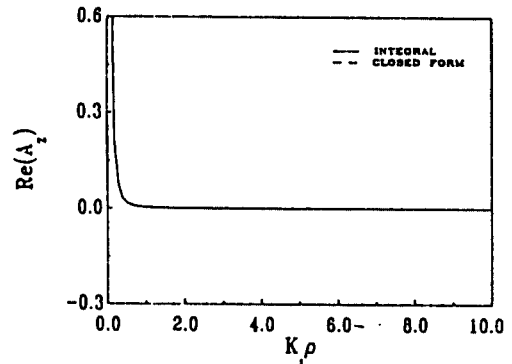
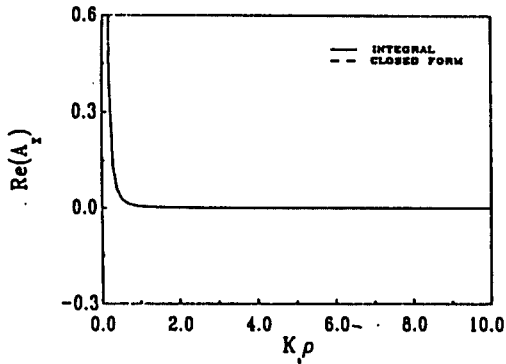
Finally, substituting the approximations (37) and (40) into (2), (3), (4) and (5) yields the closed form approximation for the microstrip surface Green's function.

The approach introduced in this section to approximate the radiation field of the continuous spectrum on a relatively thin planar grounded dielectric slab can be easily extended for the case of thick dielectric slab via Taylor-series expansion of the integrands of the imaginary parts of A_x and A_z . It is also noticed that the same argument is valid for the asymptotic approximation of the field above the dielectric surface. However, this is beyond the scope of the present paper.

IV. Numerical Results and Discussion

First, the accuracy of the approximate closed form representation of the Sommerfeld type integrals developed in the previous section is verified by comparison with the exact numerical integration results. Then, the accuracy of the approximate closed form representation for the microstrip surface Green's function is illustrated via some numerical calculations of mutual impedance between entire domain basis functions. For the numerical integration techniques employed for the computation of the Sommerfeld type integrals involved, one may refer to⁽⁹⁾.

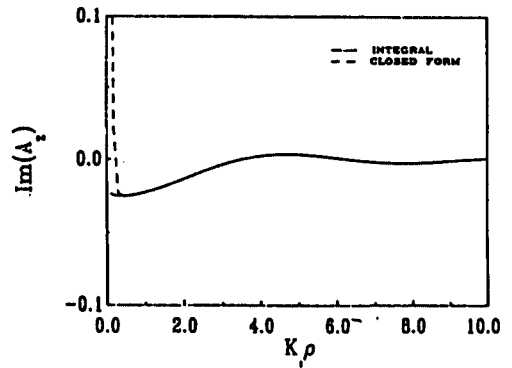
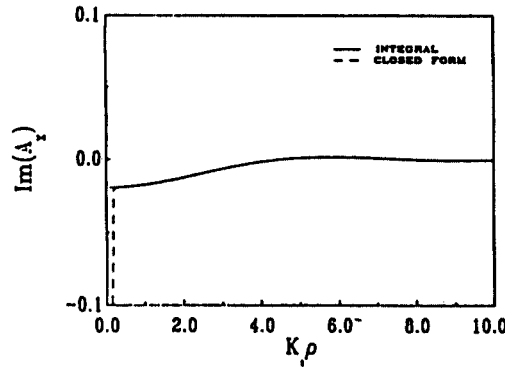
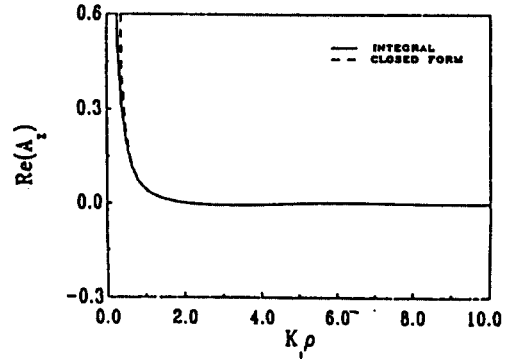
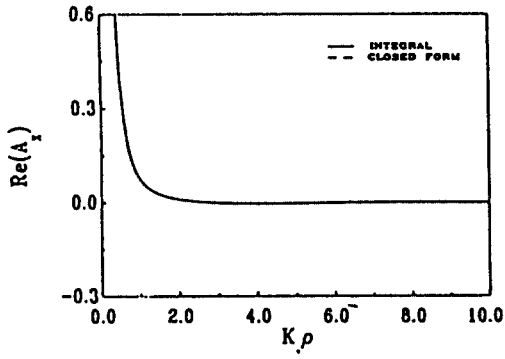
In Figure 2, the closed form approximations of the Sommerfeld type integrals are compared with the exact numerical integration results for k, ρ which varies between 0.1 and 10.0. The operating



(a)

(b)

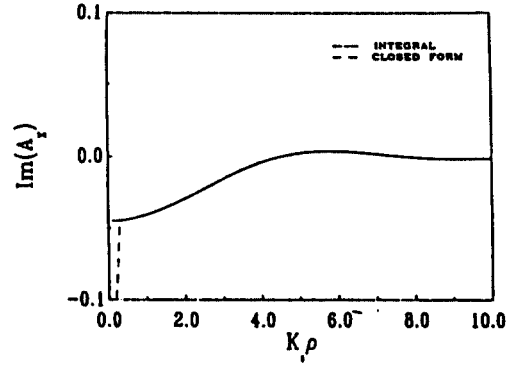
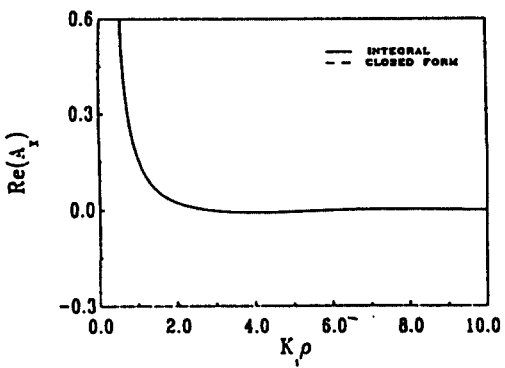
$d = 0.003175m$



(a)

(b)

$d = 0.0127m$



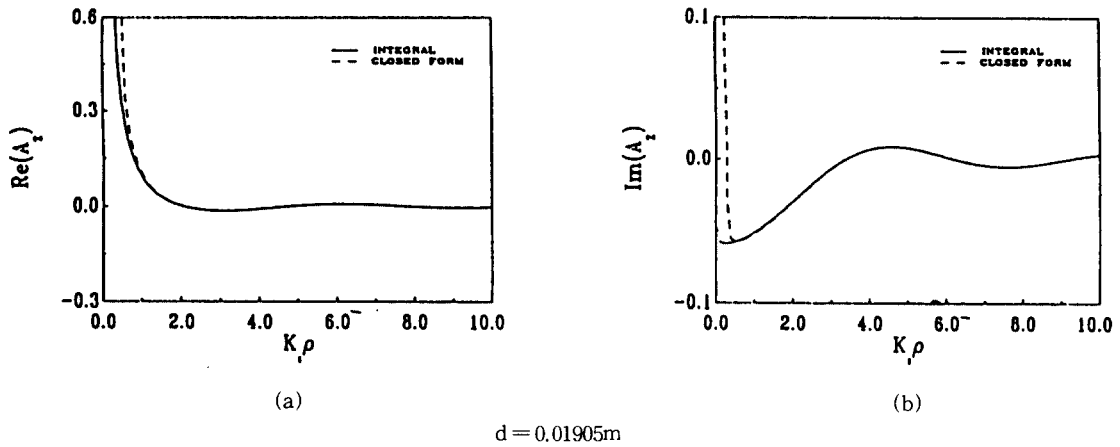


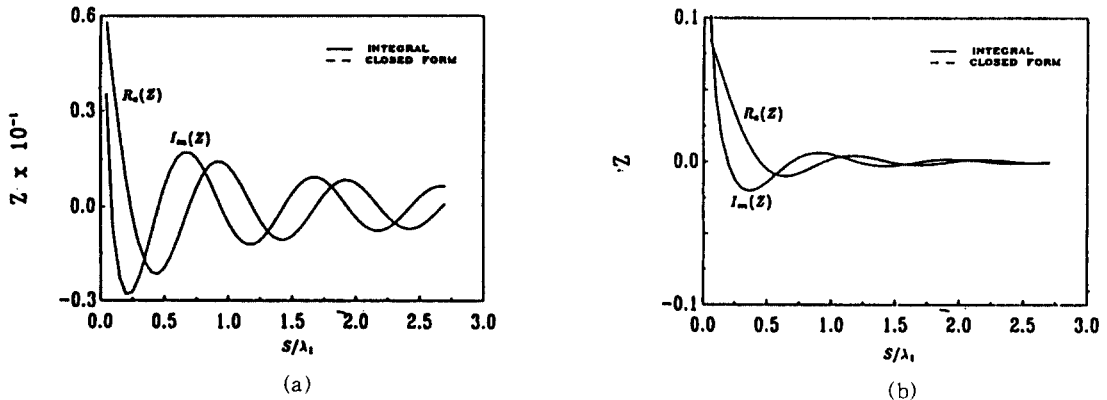
Figure 2. Comparison of the results obtained from the closed form approximation and the exact numerical integration of the Sommerfeld type integrals of (a) A_x and $\tan \delta = 0.0015$ (b) A_z ($f=633$ MHz, $\epsilon_r=2.56$, $\tan \delta=0.015$)

frequency(f), the dielectric constant(ϵ_r) and the loss tangent($\tan \delta$) are chosen to be 633MHz, 2.56, and 0.0015, respectively. In addition, the substrate thickness increases from $.0067 \lambda_1$ to $.0402 \lambda_1$.

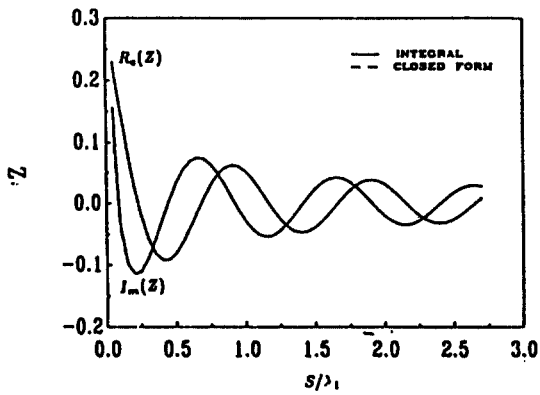
As expected, excellent accuracy is observed in both the imaginary and real parts of both A_x and A_z integrals. The slight discrepancies observed in the very close vicinity of the source is considered to be due to the strong reactive field which is not

included in the derivation of the closed approximation.

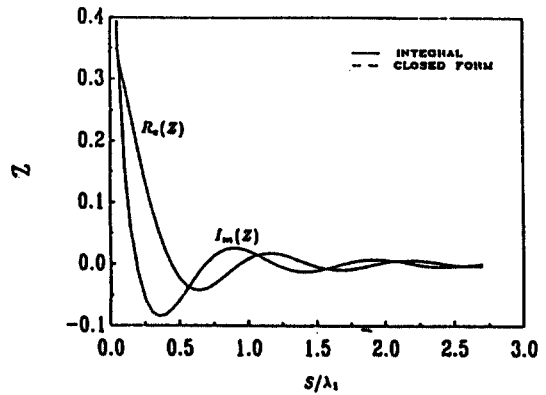
Figures 3 and 4 show the mutual impedances between two co-linear entire domain basis functions and two parallel entire domain basis functions, respectively, as a function of the spacing between basis functions relative to the free space wavelength.



$d = 0.01\lambda_1$

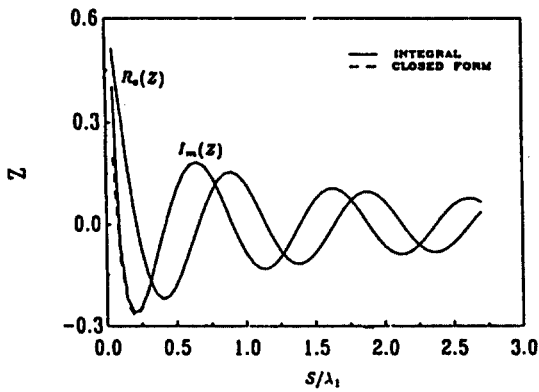


(a)

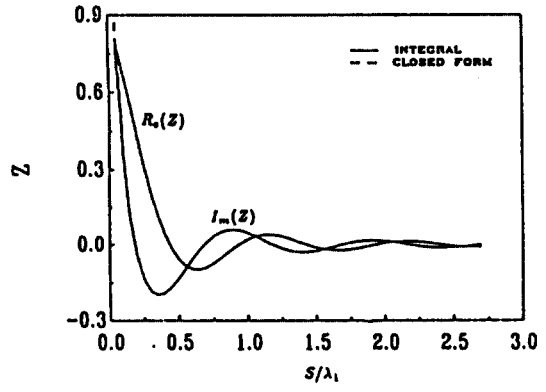


(b)

$d = 0.02\lambda_1$

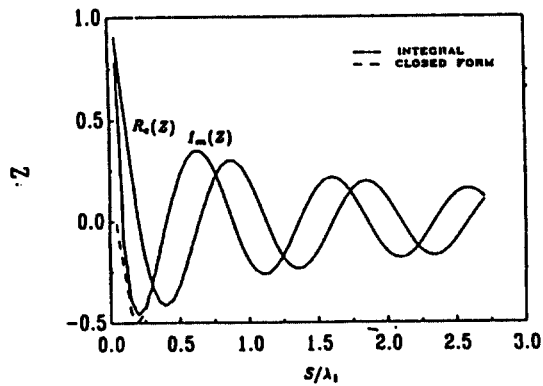


(a)

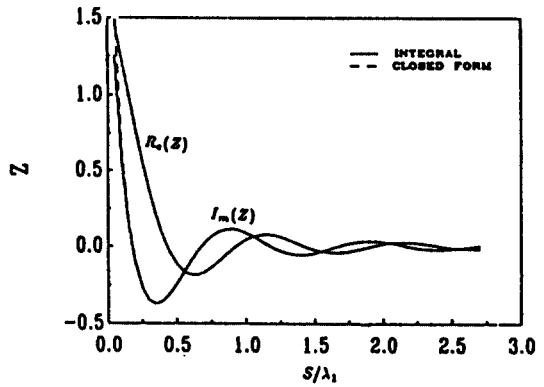


(b)

$d = 0.03\lambda_1$



(a)



(b)

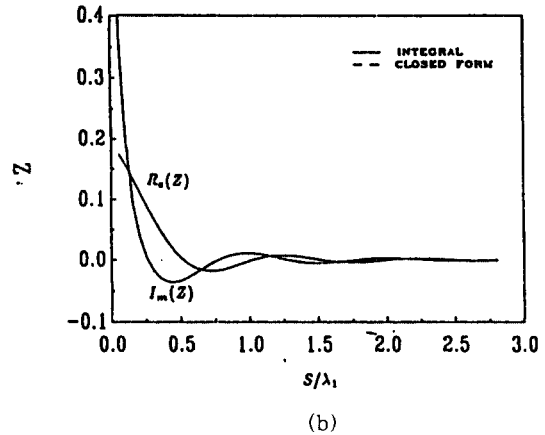
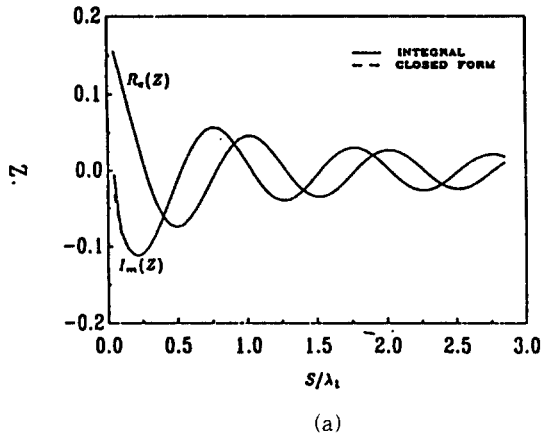
$d = 0.04\lambda_1$

Figure 3. The mutual impedance (Z) between (a) two co-linear, and (b) two parallel entire domain basis functions as a function of separation (S) relative to a free space wavelength (λ_1). ($f=300\text{MHz}$, $\epsilon_r=2.55$)

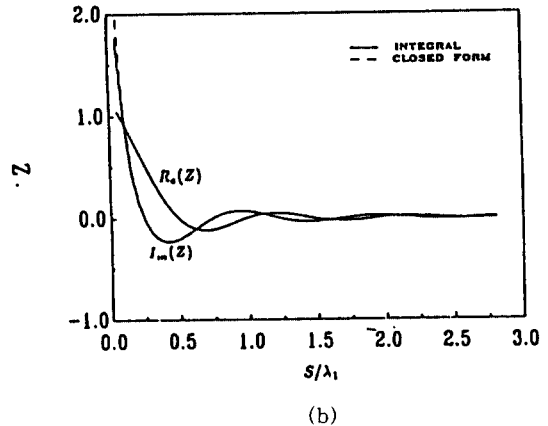
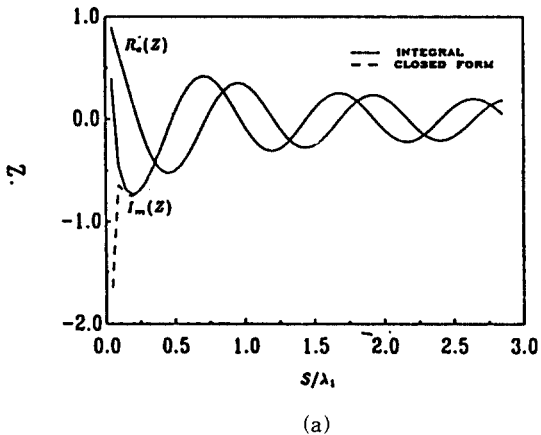
In each figure, the solid lines represent the numerical results obtained via exact numerical computation of the pertinent integrals A_x and A_z , and the discrete lines represent the results obtained via the use of the corresponding closed-form approximations. The geometry in Figure 3 consists of two identical current modes of length $0.3 \lambda_1$ and

width $0.3 \lambda_1$ on an infinite grounded dielectric substrate ($\epsilon_r=2.55$) of thicknesses $0.01 \lambda_1$, $0.02 \lambda_1$, $0.03 \lambda_1$ and $0.04 \lambda_1$.

The geometry for Figure 4 consists of two identical modes of length $0.15 \lambda_1$ and width $0.193 \lambda_1$, and the thicknesses of the substrate ($\epsilon_r=10.2$) are $0.0188 \lambda_1$, and $0.0376 \lambda_1$.



$$d = 0.0188 \lambda_1$$



$$d = 0.0376 \lambda_1$$

Figure 4.g The mutual impedance (Z) between (a) two co-linear, and (b) two parallel entire domain basis functions as a function of separation (S) relative to a free space wavelength (λ_1). ($f=300\text{MHz}$, $\epsilon_r=10.2$)

Again, the results obtained from the use of the closed-form approximation agree extremely well with the exact numerical integration results.

With regard to CPU times, the closed-form approximation takes about 3 minutes on a VAX 11 / 750 for the computation of the two mutual impedance curves(a) and (b) per each dielectric thickness in the Figures 3 and 4. However, the same computation takes about one and a half hours even though the efficient numerical integration method in [9] is used.

V. Conclusion

A simple and accurate closed form approximation has been developed for the microstrip dyadic surface Green's function required for a rigorous MM analysis of microstrip antennas. The accuracy of this approximate closed form approximation is tested, first, by comparing the results obtained for the closed form approximation and the exact numerical integration of the Sommerfeld type integrals in terms of which the microstrip surface Green's function is expressed, and then by comparing some mutual impedance calculations obtained via the closed form approximation and via the exact numerical integration. The tested dielectric constants of the grounded dielectric substrates are 2.56(1-j 0.0015), 2.55, and 10.2. In all cases, the results show that the accuracy remains to be valid even for observation points as near as $0.1 \lambda_0$ from the source point for a substrate thickness as large as $0.04 \lambda_0$, where λ_0 is the free space wavelength. As a result, the rigorous MM analysis of the microstrip antenna arrays fabricated on a relatively thin dielectric substrate of practical interest can be significantly facilitated by replacing the microstrip surface Green's function with the approximate closed form representation developed in this study. A typical CPU time on a VAX 11 / 750 required for 110 mutual impedance calculations is about 3 minutes.

Acknowledgement

The author would like to express his appreciation to Professor P.H. Pathak at the Ohio State University and Professor D.M. Pozar at the University of Massachusetts for their supports of this research and guidance.

References

1. D. M. Pozar, "Input Impedance and Mutual Coupling of Rectangular Microstrip Antennas," IEEE Trans. Antennas and Prop., Vol.AP-30, pp.1191-1196, November 1982.
2. D. M. Pozar, "A Microstrip Antenna Aperture Coupled to a Microstrip Line," Electronics Letters, Vol.21, pp.48-50, January 17, 1985.
3. D. M. Pozar, "Analysis of Finite Phased Arrays of Printed Dipoles," IEEE Trans. Antennas and Prop., Vol.AP-33, pp.1045-1053.
4. D. M. Pozar, "Finite Phased Arrays of Rectangular Microstrip Patches," IEEE Trans. Antennas and Prop., Vol.AP-34, pp.658-665, May 1986.
5. R. F. Harrington, *Time Harmonic Electromagnetic Fields*, McGraw-Hill, New York, 1969.
6. R. E. Munson, "Conformal Microstrip Antennas and Microstrip Phased Arrays," IEEE Trans. Antennas and Prop., Vol.AP-22, pp. 74-77; January 1974.
7. R. E. Collin and F. J. Zucker, Eds., *Antenna Theory*, McGraw-Hill, New York, 1969.
8. L. B. Felsen and N. Marcuvitz, *Radiation and Scattering of waves*, Prentice-Hall, New Jersey, 1973.
9. Ikguen Choi, An Approach for Efficient Numerical Integration of the Sommerfeld Type Integrals Pertinent to the Microstrip Green's Function, the Journal of the Korean Institute of Communication Sciences, Vol.18, No.1, pp. 143-149, January 1993.



崔翼權(Ik Guen Choi) 정회원

1950년 12월 26일생

1974년 2월 : 서울대학교 공과대학
자원공학과(공학사)

1976년 2월 : 서울대학교 대학원 자
원공학과(공학석사)

1986년 9월 : 미국 오하이오주립대
학교 대학원 전자공학
과(공학박사)

1976년 3월 ~ 1979년 6월 : 육군 제3사관학교 교수부 물리
학 전임강사

1981년 10월 ~ 1986년 9월 : 미국 오하이오주립대학교 ESL
(Electro Science Laboratory)
연구원

- 지하구조물 탐사용 레이더시스템개발연구

- 마이크로스트립 어레이 안테나개발연구

1986년 10월 ~ 1987년 9월 : 미국 마사추세츠주립대학교
Antenna Laboratory 연구원

- 마이크로스트립 웨이스트 어레이 안테나
연구

1987년 10월 ~ 현재 : 한국 전자통신연구소 이동통신기술연
구단

- 위성추적레이더 시스템 성능분석연구

- 식별부호 자동 송출 및 수신시스템 개발연
구

- 특수 페이지개발연구

- 이동통신용 소형내장형안테나개발 및 전
파특성연구

- EMI / EMC 측정 및 방지대책연구